

## SS433 in the ultraviolet<sup>★</sup>

J.F. Dolan<sup>1</sup>, P.T. Boyd<sup>1,2</sup>, S. Fabrika<sup>3</sup>, S. Tapia<sup>3</sup>, V. Bychkov<sup>3</sup>, A.A. Panferov<sup>3</sup>, M.J. Nelson<sup>4</sup>, J.W. Percival<sup>4</sup>, G.W. van Citters<sup>5</sup>, D.C. Taylor<sup>6</sup>, and M.J. Taylor<sup>7</sup>

<sup>1</sup> Laboratory for Astronomy & Solar Physics NASA Goddard Space Flight Center, Greenbelt, MD 20771 USA

<sup>2</sup> Universities Space Research Association @ NASA Goddard Space Flight Center, Greenbelt, MD 20771 USA

<sup>3</sup> Special Astrophysical Observatory, Nizhnij Arkhyz, Karachai-Cherkess Republic, 357147, Russia

<sup>4</sup> Department of Astronomy & Space Astronomy Laboratory, University of Wisconsin, Madison, WI 53706 USA

<sup>5</sup> Division of Astronomical Sciences, National Science Foundation, 4201 Wilson Blvd., Arlington, VA 22230 USA

<sup>6</sup> Space Telescope Science Institute, 3700 San Martin Drive, Baltimore, MD 21218 USA

<sup>7</sup> Department of Physics and Engineering, Loras College, P.O. Box 178, Dubuque, IA 52004 USA

Received 2 April 1997 / Accepted 27 June 1997

**Abstract.** The High Speed Photometer (HSP) on the Hubble Space Telescope observed SS433 at 15 different epochs between 1993 May and November. Polarimetric observations were obtained in a 340 Å FWHM bandpass centered at 2770 Å; photometric observations were made in a bandpass extending between 1400 and 3000 Å. The polarization in the UV is both large ( $\langle p \rangle = 13 \pm 4\%$ ) and variable. Observations at the 6-m telescope of the Special Astrophysical Observatory find the polarization in the U band to be intermediate in magnitude between that in the V band and that we detect in the UV. These results are best explained by the existence of a Rayleigh scattering component in the polarized radiation. Less than 1.2% of the flux from SS433 between 1400 and 3000 Å is modulated with a period between 200  $\mu$ s and 100 s at 164-d phase  $\psi = 0.131$ , when the two sets of emission lines in the SS433 spectrum have a local maximum in the separation of their redshifts.

**Key words:** polarization – stars: individual: SS433 – ultraviolet: stars

### 1. Introduction

SS433 is an emission-line binary system in a class by itself (Krumenaker 1975; Stephenson & Sanduleak 1977; Margon 1984). Two sets of emission lines in its spectra show relativistic Doppler shifts in opposite directions corresponding to a mass motion velocity  $v/c = 0.26$ . The two sets of lines vary regularly in redshift with a 164-d period ascribed to the precession of two counter-directed beams. (The best estimate of the 164-d period is now 162.5 d.) We adopt here the

164-d phase,  $\psi$ , of Margon & Anderson (1989):  $E(\psi) = \text{JD}(2, 443, 562.37 \pm 0.30) + (162.50 \pm 0.03)\psi$ , where  $E(\psi)$  is the epoch at which the two sets of lines have the same redshift at integer values of  $\psi$ . The lines have maximum redshift separation at 164-d phase  $\psi = 0.631$ . A smaller maximal separation occurs at  $\psi = 0.131$ , and a second epoch of redshift equality at  $\psi = 0.262$ . The system also exhibits a 13-d period in photometric and spectroscopic observations, originally discovered as a 6 day spectroscopic period (Newsom & Collins 1981). The 13-d period is attributed to orbital motion and eclipse phenomena in the binary (Cherepashchuk 1981; Stewart et al. 1987). We adopt here the 13-d phase,  $\phi$ , of Goranskij et al. (private communication) relative to photometric minimum at integer values of  $\phi$ :  $E(\phi) = \text{JD}(2, 450, 023.69 \pm 0.26) + (13.08231 \pm 0.00021)\phi$ .

Variable (and hence, intrinsic) linear polarization in the radiation from SS433 has been detected in the visible, both broadband (McLean & Tapia 1980) and in the B, V, R, and I bandpasses (Efimov et al. 1984). Repetitive polarimetric variability exists on both the 13-d and 164-d time scales. The magnitude of the observed polarization,  $p$ , which is the sum of the intrinsic and interstellar polarization, ranges between  $\sim 1\%$  and  $\sim 3\%$ , with an equatorial position angle,  $\theta$ , near  $175^\circ \pm \sim 15^\circ$ . McLean & Tapia (1980) discuss mechanisms that can produce the optical polarization and conclude that Thomson scattering from free electrons is the most probable cause. No circular polarization has been detected in the visible (normalized Stokes parameter  $v < 0.1\%$ ) (Liebert et al. 1979; Michalsky et al. 1980). The linear polarization at 2.2  $\mu$ m in the far IR is also  $< 0.1\%$  (Thompson et al. 1979). SS433 is strongly reddened:  $A_V = 7.8 \pm 0.5$  (Wagner 1986 and references therein). The interstellar polarization in the direction of the source ( $l = 39^\circ, b = -2^\circ$ ) is not well determined as a function of distance. McLean & Tapia (1980) estimate the interstellar polarization  $p_i$  in the visible is  $1.5\% \leq p_i \leq 2.7\%$  at  $\theta_i = 30^\circ$ , based on (i) the polarization exhibited by stars in the field, and (ii) the upper limit on the po-

Send offprint requests to: J.F. Dolan

<sup>★</sup> Based in part on observations with the Hubble Space Telescope obtained at the Space Telescope Science Institute, which is operated by AURA, Inc. under NASA contract NAS5-26555.

larization at  $2.2 \mu\text{m}$  together with the wavelength dependence of the standard interstellar polarization curve, which has a maximum at  $5500 \text{ \AA}$  (Serkowski 1974). Michalsky et al. (1980) derive an interstellar polarization twice as large in the visible as that of McLean & Tapia (1980) by assuming that all the polarization in SS433 is interstellar, an assumption which the observed variability demonstrates is incorrect. Efimov et al. (1984) derive the interstellar polarization from the observed polarization of SS433 alone. Efimov et al. assume that any intrinsic polarization is independent of wavelength (like Thomson scattering), though it can vary with time, and they use the wavelength dependence of the observed polarization together with the wavelength dependence of the standard interstellar polarization curve to separate out an interstellar polarization component. Efimov et al. find an interstellar polarization which peaks at  $p_i = 4.69 \pm 0.02\%$  at  $5860 \text{ \AA}$ , but report their data is also consistent with a maximum interstellar polarization as low as  $2.81 \pm 0.13\%$  peaking at  $5000 \text{ \AA}$ . All solutions have  $\theta_i = 3.6^\circ \pm 2.8^\circ$ . If the interstellar polarization is as large in the visible as any of these values reported in the literature, then the polarization and position angle of the radiation emitted by SS433 in the visible must be significantly different from that observed at the Earth. The standard interstellar polarization curve (Serkowski 1974), however, predicts that  $p_i < 2.5\%$  at  $2770 \text{ \AA}$  for any of these estimates.

The radiation from SS433 in the radio region of the spectrum is strongly polarized (Hjellming & Johnston 1981; Niell et al. 1981),  $p = 8 - 20\%$  with  $\theta = 100^\circ \pm 20^\circ$ . The polarization occurs in jet-like linear structures on both sides of the central radio source, which is coincident with the optical image. The position angle of the jets varies approximately sinusoidally with the 164-d precession period about a mean value of  $100^\circ \pm 2^\circ$  with an amplitude of  $19^\circ \pm 3^\circ$ . The radio emitting material appears to propagate away from the central source in discrete packets. Radio observers have assumed these “blobs” possess the same semi-relativistic velocity ( $v/c = 0.26$ ) as those producing the redshifted optical emission lines in order to determine a distance to the source of  $5.1 \pm 0.5 \text{ kpc}$  (Hjellming & Johnston 1981).

## 2. Observations

The High Speed Photometer (HSP) was one of the four original axial instruments on board the Hubble Space Telescope. A description of the HSP is given by Bless et al. (1992). Polarimetric observations were obtained in the F277M bandpass, defined by a  $340 \text{ \AA}$  wide filter (FWHM response to a flat incident spectrum) centered at  $2770 \text{ \AA}$ , using a  $0.65''$  diameter aperture. The polarization of the radiation from SS433 was determined from its counting rate in four different analyzers, oriented at  $0^\circ$ ,  $45^\circ$ ,  $90^\circ$ , and  $135^\circ$  in position angle relative to an internal coordinate system. Multiple measurements were combined into a single set of counting rates for each orientation. The normalized Stokes parameters and their associated uncertainties were then derived by the procedure outlined by Dolan et al. (1994). Wolinski et al. (1996) showed that polarimetric precisions  $\sigma(q, u) \sim 0.3\%$  were routinely attainable on measurements of the normalized Stokes parameters  $q$  and  $u$  with

**Table 1.** UV Polarization of SS433

JD (244+)	$\psi$	$\phi$	$p(\%)$	$\theta(\text{deg})$
9126.510	(34).241	(0).420	$5 \pm 12$	$71 \pm 21$
9128.395	.252	.564	$26 \pm 10$	$38 \pm 11$
9130.603	.266	.733	$0 \pm 12$	$72 \pm 45$
9133.135	.282	.927	$23 \pm 13$	$45 \pm 20$
9216.946	.797	(7).333	$15 \pm 07$	$111 \pm 15$
9235.157	.909	(8).725	$13 \pm 09$	$137 \pm 13$
9262.261	(35).076	(10).797	$21 \pm 10$	$102 \pm 17$
9285.961	.222	(12).609	$35 \pm 10$	$79 \pm 08$
9288.702	.239	.818	$36 \pm 17$	$66 \pm 08$
9290.442	.250	.951	$0 \pm 16$	$5 \pm 34$
9290.639	.251	.966	$0 \pm 15$	$61 \pm 35$
9292.651	.263	(13).120	$11 \pm 14$	$90 \pm 27$
9294.859	.277	.289	$22 \pm 09$	$87 \pm 12$
9306.908	.351	(14).210	$22 \pm 09$	$71 \pm 17$

the HSP. Rotation of the measured Stokes parameters to the equatorial co-ordinate system is done by adding the equatorial position angle of the  $0^\circ$  analyzer during the observation to the position angle derived in the internal coordinate system of the polarimeter. The polarization and position angle, and their associated uncertainties, were derived from the Stokes parameters using the relationships given by Dolan & Tapia (1986). The magnitude of polarization was corrected for its non-normal distribution at low statistical significance (Simmons & Stewart 1985) using the correction factor of Wardle & Kronberg (1974). No correction was made to the measured position angle because it is an unbiased estimator of the true position angle (Wardle & Kronberg 1974). To derive the flux density in the F277M bandpass, we used the average of the summed count rates in the  $0^\circ + 90^\circ$  orientation analyzers and the summed count rates in the  $45^\circ + 135^\circ$  pair (Dolan et al. 1994).

The HSP observed SS433 polarimetrically on the 14 epochs listed in Table 1. The 13-d and 164-d phases at these epochs are also given in the table. The epochs were chosen to investigate the polarimetric variability associated with both the 13-d and 164-d periods. Two series of observations at two day intervals were taken at approximately the same 164-d phase,  $\psi \sim 0.25$ , to investigate the 13-d variability.

Photometric observations were also obtained in the F140LP filter on 1993 October 11 using a  $1.0''$  aperture. The F140LP bandpass extends between  $1400$  and  $3000 \text{ \AA}$ , but because of heavy reddening in the direction of SS433, most of the detected flux must have been in the longer wavelength region of this bandpass. The  $1,035 \text{ s}$  observation, starting at JD  $2,449,271.901$ , used a  $10.7 \mu\text{s}$  sample time to search for any periodic signal in the flux. The system was at 164-d phase  $\psi = (35).131$ , where the two sets of emission lines have a local maximum in the separation of their redshifts, and 13-d phase  $\phi = 0.534$ .

## 3. Results

### 3.1. UV polarimetry

To allow comparison with the results of McLean & Tapia (1980) and Efimov et al. (1984), we present UV results both as  $p$  and

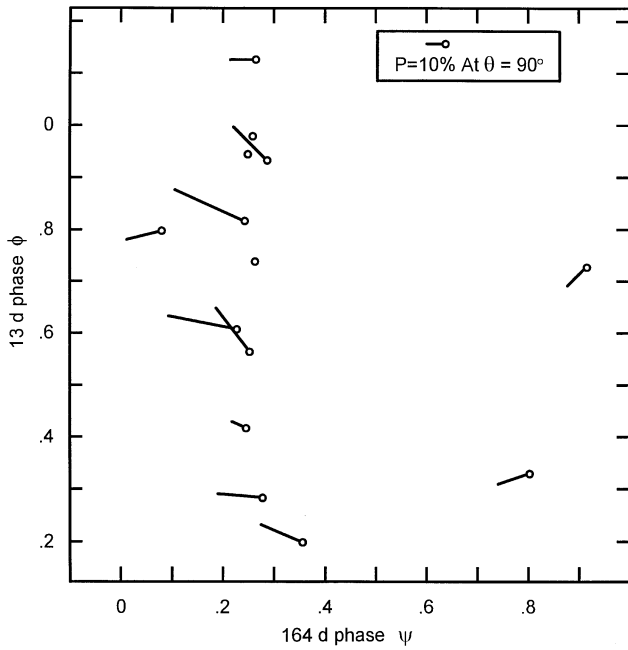


**Fig. 1.** The polarization of SS433 in the F277M bandpass at the 14 epochs from 1993 May to November given in Table 1. Observations were obtained at the 164-d phase given on the abscissa and the 13-d phase given on the ordinate. The fractional polarization is proportional to the length of the vector attached to each data point; the length corresponding to a polarization of 10% is shown. Each polarization has been corrected for its non-normal distribution at low statistical significance using the correction factor of Wardle & Kronberg (1974). The position angle of the vector (N is up, E is to the left) is the equatorial position angle of the polarization.

$\theta$ , and in the form of the normalized Stokes parameters in the equatorial co-ordinate system,  $q$  and  $u$ . The polarization and position angle of the UV radiation we observed from SS433 (Table 1), uncorrected for any (constant) value of the interstellar polarization in the UV, are shown in Fig. 1 as a function of both 13-d and 164-d phase. The normalized Stokes parameters from which  $p$  and  $\theta$  were derived are shown in Fig. 2 as a function of 13-d phase. The mean values of the Stokes parameters we measured,  $\langle q \rangle = -12 \pm 3\%$ ,  $\langle u \rangle = 5 \pm 4\%$ , are larger than the normalized Stokes parameters in the visible (always  $< 3\%$ ). The normalized Stokes parameters are nearly Gaussian in their distribution (Clark et al. 1983), with their deviation from a normal distribution “hardly affecting the standard determination of confidence intervals”. Hence, we may test the normalized Stokes parameters for variability about their mean with the  $\chi^2$  test.  $\chi^2$  is 24.1 (19.1) for  $u$  ( $q$ ), a value exceeded by only 3% (12%) of all random distributions having 13 degrees of freedom and the same mean and variance as our observations. Stokes parameter  $u$  is variable at the 95% level of confidence. The variability observed in  $u$  is  $> 20\%$  from maximum to minimum, again much larger than the variability observed in the visible. The mean normalized Stokes parameters give  $\langle p \rangle = \sqrt{\langle q \rangle^2 + \langle u \rangle^2} = 13 \pm 4\%$ . The mean polarization in the UV is significantly larger than that observed in the

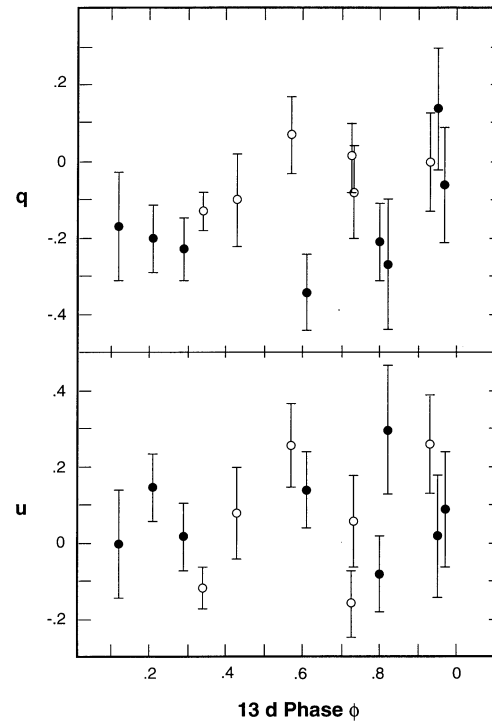


**Fig. 2.** The normalized Stokes parameters observed from SS433 in the F277M bandpass as a function of 13-d phase. Open circles denote observations obtained during orbit 34 of the 164-d ephemeris given in the text; filled circles, orbit 35. The error bars represent  $\pm 1\sigma$  uncertainties. Above:  $q$ ; below:  $u$

visible. (The weighted mean value of the polarization from the data in Table 1 is  $\bar{p} = 18 \pm 3\%$ .  $\langle p \rangle$  is preferred as a measure of the mean polarization because  $p$  is not normally distributed [Simmons & Stewart 1985].)

The position angles of the non-zero polarizations we observed are shown in Fig. 3 as a function of 164-d phase. Only position angles for the non-zero polarizations (after the Wardle and Kronberg correction) are shown because the  $1\sigma$  uncertainty on the position angle rapidly approaches  $\pm 45^\circ$  as  $p/\sigma(p)$  becomes  $< 1$  (Wardle & Kronberg 1974).  $\theta$  is an unbiased best estimator of the position angle of the polarization;  $\bar{\theta} = 79^\circ \pm 8^\circ$  for the data in Fig. 3.  $\langle \theta \rangle$ , the mean value derived from  $\langle q \rangle$  and  $\langle u \rangle$ , also equals  $79^\circ \pm 8^\circ$  for all 14 observations in Table 1.  $\theta$  is not distributed normally, but the value of  $\chi^2$  for the data in Fig. 3 about  $\bar{\theta}$  is 47 for 10 degrees of freedom. Because the  $\chi^2$  test is robust against non-normally distributed data (Meyer 1986), this large a value of  $\chi^2$  confirms the existence of the variability seen in Fig. 3.

### 3.2. Polarization in the visible

Observations which rule out the possibility that the polarization in the visible changed between the epoch of its last reported previous observation (over a decade ago) and the epoch of our UV observations were obtained at the 6-m telescope of the Special Astrophysical Observatory using the Minipol polarimeter

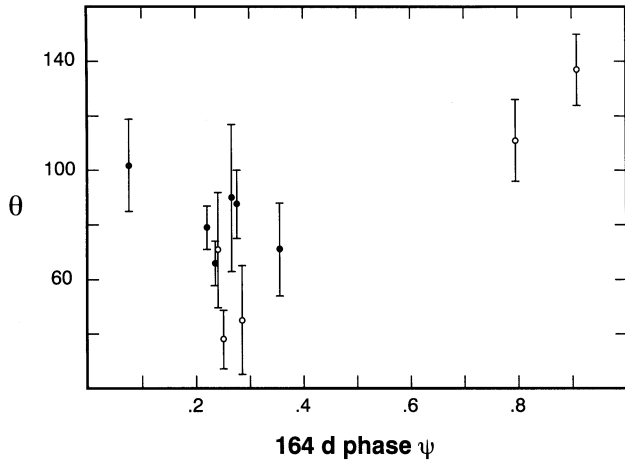


**Fig. 3.** The equatorial position angle of the UV flux from SS433 when the polarization was non-zero, as a function of 164-d phase. Open circles denote observations obtained during orbit 34 of the ephemeris given in the text; filled circles, orbit 35. The error bars represent  $\pm 1\sigma$  uncertainties on the position angle as propagated from the uncertainties on the normalized Stokes parameters.

**Table 2.** Polarization of SS433 in the Visible

JD (245+)	bandpass	Observed		Intrinsic	
		p(%)	$\theta$ (deg)	p(%)	$\theta$ (deg)
0319.242	U	$7.1 \pm 0.7$	$93 \pm 3$	$8.9 \pm 0.9$	$90 \pm 10$
0319.257	B	$3.08 \pm 0.14$	$161 \pm 1$	$2.6 \pm 0.4$	$141 \pm 16$
0319.262	V	$2.04 \pm 0.02$	$157 \pm 1$	$2.2 \pm 0.4$	$92 \pm 18$
0319.269	R	$2.49 \pm 0.03$	$162 \pm 1$	$2.1 \pm 0.4$	$139 \pm 20$
0319.275	I	$2.07 \pm 0.03$	$160 \pm 1$	$1.9 \pm 0.3$	$136 \pm 14$

on 1996 August 24. The polarization we observed in the B, V, R, and I bands at phases  $\psi = 0.581$  and  $\phi = 0.59$  (Table 2) is consistent with all previous measurements in the visible, being  $< 3\%$  at  $\theta \sim 160^\circ$ .

The polarization we observe in the U band is significantly larger than that in the visible, and intermediate in magnitude between that in the B to I bands and that we observed at 2770 Å. The position angle we observed in the U band ( $93^\circ \pm 3^\circ$ ) is also in the range of those we observed in the UV (cf. Fig. 3), and differs significantly from that we observed in the B to I bands ( $\langle \theta \rangle = 160^\circ \pm 1^\circ$  in these four bands). Because the observed polarization has normalized Stokes parameters  $q = q_i + q_o$ , where  $q_i$  is the interstellar component and  $q_o$  is the intrinsic component (and likewise for  $u$ ), and because interstellar polarization decreases in magnitude at shorter wavelengths, our observations require that the intrinsic component of polarization in SS433 must increase in magnitude as wavelength decreases. The difference between our UV results and the polarization previously reported in the visible is caused by a wavelength dependence of the polarization in SS433 rather than a temporal variation in its polarized flux.

We also observed the polarization of background stars in the near vicinity of SS433. Using the nomenclature of Leibowitz & Mendelson (1982), we find S16 has  $p(V) = 1.54 \pm 0.06\%$  at

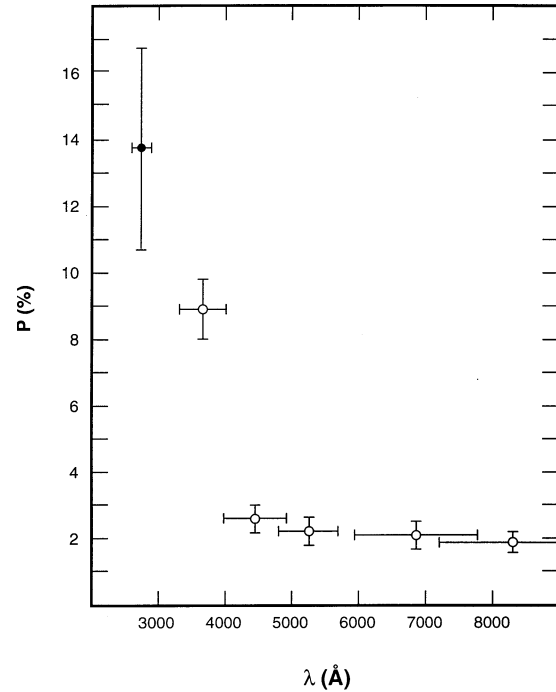


**Fig. 4.** The intrinsic polarization of SS433 as a function of wavelength, derived from the observed polarization by vector subtraction of the interstellar polarization predicted by the phenomenological model of Serkowski (1974) using  $p_i(\text{max}) = 2.1 \pm 0.6\%$ ,  $\theta_i = 10^\circ \pm 10^\circ$ , and  $\lambda(\text{max}) = 5240 \text{ \AA}$ . The open circles are derived from the data in Table 2; the filled circle is derived from the mean of the data in Table 1. The vertical error bars represent  $\pm 1\sigma$  uncertainties on the polarization as propagated from the uncertainties on the observed Stokes parameters and the assumed interstellar polarization; the horizontal error bars demarcate the FWHM of the observational bandpass for a flat incident spectrum.

$\theta(V) = 13^\circ \pm 1^\circ$  and  $p(B) = 2.1 \pm 0.2\%$  at  $\theta(B) = 8^\circ \pm 2^\circ$ ; and S1 has  $p(B) = 1.5 \pm 0.1\%$  at  $\theta(B) = 3^\circ \pm 2^\circ$ . McLean & Tapia (1980) report that S2 has  $p = 1.52 \pm 0.09\%$  at  $\theta = 35^\circ \pm 2^\circ$  and S3 has  $p = 1.2 \pm 0.2\%$  at  $\theta = 16^\circ \pm 5^\circ$  in a broad bandpass with an effective center near 7000 Å. The angular distance of these background stars from SS433 ranges from  $33''$  to  $100''$  both N and S of it. These results are consistent with the interstellar polarization in the direction of SS433 derived by McLean & Tapia (1980),  $p_i = 2.1 \pm 0.6\%$ , but with  $\theta_i$  closer to  $10^\circ$  than  $30^\circ$ . If we subtract from our observed values of polarization the polarizations predicted as a function of wavelength by the standard phenomenological model of interstellar polarization (Serkowski 1974), we can derive an estimate of the intrinsic polarization in the radiation emitted by SS433. Using  $p_i(\text{max}) = 2.1 \pm 0.6\%$ ,  $\theta = 10^\circ \pm 10^\circ$ , and  $\lambda(\text{max}) = 5240 \text{ \AA}$  for the interstellar polarization in the direction of SS433 gives the estimates of the intrinsic polarization listed in Table 2. The intrinsic polarization we estimate in the F277M bandpass is  $\langle p_o \rangle = 13.7 \pm 3.0\%$  at  $\langle \theta_o \rangle = 81^\circ \pm 10^\circ$ . The wavelength dependence of the intrinsic polarization we estimate is shown in Fig. 4.

It is important to remember that the polarization from SS433 is variable, and that the intrinsic polarization we estimate at

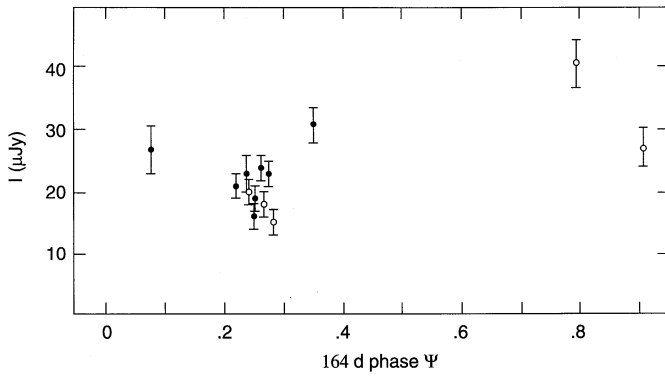


**Fig. 5.** The flux density observed from SS433 in the F277M bandpass during the polarimetric measurements in Table 1 as a function of 164-d phase. The symbols are the same as in Fig. 3.

2770 Å is the mean of 14 different observations taken at epochs (and phases) different from the epoch (and phase) of the 6-m observations. Even so, an increase in polarization with decreasing wavelength is clear. Previous observations (McLean & Tapia 1980; Efimov et al. 1984) show temporal variability of the polarization in the wavelength region covered by the bandpasses from B to I, with  $\Delta p$  ranging from  $\sim 1\%$  to  $\sim 2\%$ . The intrinsic polarization from SS433 in these bandpasses must then be at least as large as  $\Delta p$ . The magnitude of the intrinsic polarization we estimate in the B to I bands (Table 2) is as large as the  $p$  observed in every bandpass, and so is consistent with previous observations.

### 3.3. UV photometry

The flux densities in the F277M bandpass observed from SS433 during our polarimetric measurements are shown in Fig. 5 as a function of 164-d phase. The flux density is variable:  $\chi^2 = 67$  for 13 degrees of freedom about the weighted mean,  $\langle S_\nu \rangle = 21.0 \pm 1.4 \mu\text{Jy}$ . The UV variability is consistent with the variability observed in the visible (Panferov et al. 1997): a bright state which occurs near the phase of maximum redshift separation of the two sets of emission lines in the spectrum ( $\psi = 0.8 \pm 0.05$ ) at the binary phase of greatest elongation ( $\phi = 0.3 \pm 0.15$ ), and a low state which occurs when the accretion disk around the X-ray source is nearly edge on (when  $\psi = 0.27 \pm 0.1$  and  $\phi = 0.0 \pm 0.2$ ). Under these criteria, SS433 was in the bright state on JD 2,449,216 (cf. Table 1), and in the low state on (JD 244) 9133, 9288, 9290 (both observations) and 9292.

We detected  $2.08 \pm 0.05 \text{ count s}^{-1}$  from SS433 in the F140LP bandpass, equivalent to a flux density of  $7.8 \pm 0.2 \mu\text{Jy}$  for a source with an observed spectrum in this bandpass similar to that of the calibration source BD +75° 325, an O5p star. SS433 is heavily reddened, however, and so its observed spectrum is unlikely to resemble that of the calibration star over this wide a bandpass. We searched for the existence of a periodic signal in this data by using the standard auto-correlation function (ACF) and power-spectrum (PSF) techniques (Perci-

val et al. 1995). We also searched for a signal with time-varying frequency during our observation by using the Gabor transform (Boyd et al. 1995), a type of short time-windowed Fourier transform. The data were consistent with a time series having only random variations about its mean under all tests we performed. To estimate our sensitivity to a periodic signal, we added an artificial signal to the data with a 10% random probability of having a detected photon at every phase zero of its 0.5 s period, a count rate of  $0.21 \text{ counts s}^{-1}$ . We detected this artificial signal at the  $8\sigma$  level of significance in both the ACF and PSF analyses. Based on this result, we estimate as a  $3\sigma$  upper limit that  $< 1.2\%$  of the flux from SS433 was pulsed with a period between  $200 \mu\text{s}$  and  $100 \text{ s}$  in the F140LP bandpass during our observation.

## 4. Discussion

### 4.1. Polarization

The polarization we observe in the F277M bandpass is much larger than the interstellar polarization expected in the UV toward SS433. The position angle and  $u$  Stokes parameter are both variable, further evidence that an intrinsic component of polarization is dominant in the UV. After subtracting the interstellar polarization, the ratio of the intrinsic polarization in the UV to that in the visible from SS433 is

$$\begin{aligned} \rho &= \langle p_0(UV) \rangle / \langle p_0(V) \rangle \\ &\sim \langle p_0(UV) \rangle / p_0(V) \\ &= 6 \pm 2. \end{aligned} \quad (1)$$

Efimov et al. (1984) derived a value for the interstellar polarization by assuming that the intrinsic component of polarization in SS433 was wavelength independent, which implies  $\rho = 1$ . Because  $\rho > 1$ , this assumption is incorrect. This is the cause of the difference between the interstellar polarization we find in the direction of SS433 and that derived by Efimov et al.

Given that scattering is the mechanism producing the intrinsic polarization from SS433 in the visible (McLean & Tapia 1980; Efimov et al. 1984), it is reasonable to ascribe the UV polarization to scattering as well. The cross-section for Thomson scattering,  $\sigma_T$  per free electron, is wavelength independent at optical frequencies, however. If the mechanism producing the UV polarization were solely Thomson scattering, then three emission components would be required in the spectrum of SS433: the unscattered, unpolarized component; the scattered, polarized component; and an additional scattered, polarized component in the UV whose unscattered, unpolarized radiation was not visible from the Earth. This would require an additional emission component in the UV spectrum of SS433, and we have no evidence for the existence of such a component. Fe line blanketing depolarizes pure electron scattering polarization in the UV (Bjorkman et al. 1991; Bjorkman & Bjorkman 1994) and so can not produce polarization which increases in the UV from Thomson scattering. It is difficult to reconcile the wavelength dependence of polarization we observe with Thomson scattering as the sole polarizing mechanism.

We believe our results are best explained by the existence of a Rayleigh scattering component in the polarized radiation from SS433. The existence of Rayleigh scattering would imply that a region containing neutral (recombined) atoms is present in the SS433 system. The cross-section for Rayleigh scattering per atomic electron is

$$\sigma_R = \sigma_T(\lambda_0/\lambda)^4 \quad (2)$$

for  $\lambda^2 \gg \lambda_0^2$ , where  $\lambda_0$  is the wavelength of the principal resonance line in the atomic species doing the scattering (Lyman  $\alpha$  in H).  $\sigma_R$  is 16 times larger at 2770 Å than at 5500 Å, so  $\rho$  would equal 16 if Rayleigh scattering were the sole mechanism producing the polarization. Because  $1 < \rho < 16$ , both Rayleigh and Thomson scattering mechanisms must contribute to the intrinsic polarization. Both ionized and recombined material are present in the SS433 system, so the existence of both Rayleigh and Thomson scattering is reasonable. Polarization produced by combined Rayleigh and Thomson scattering is a common feature in X-ray binary systems (Wolinski et al. 1996). Scattering regions with neutral (recombined) hydrogen can exist even in high-luminosity, X-ray emitting systems (Mason et al. 1974; Kitamoto et al. 1984).

The scattering region in SS433 can not be located in the precessing jets, which are oriented at position angle  $100^\circ \pm 20^\circ$  on the sky (Hjellming & Johnson 1981). If the polarization is caused by radiation from a central source being scattered off these jets, it would have a position angle perpendicular to the position angle of the jets, at  $\theta \sim 10^\circ \pm 20^\circ$ . (We assume here that the scattering region is not optically thick.) The position angle of the intrinsic polarization in the UV,  $\langle \theta_0 \rangle = 81^\circ \pm 10^\circ$ , is nearly parallel to the position angle of the jets in SS433. If the UV polarization is caused by scattering, then the structure doing the scattering must be oriented orthogonal to the jets. We note that models of the jets usually have them oriented perpendicular to an accretion disk around SS433 irrespective of whether the central source is a neutron star or a black hole (Fabrika 1993; Panferov & Fabrika 1993; Arav & Begelman 1993; Rose 1995). Based on previous observations, Fabrika (1993) shows that SS433 should possess an extended disk of neutral material in the plane of the accretion disk. Radiation from a central source which is scattered off material in this plane would naturally possess polarization with the position angle we detect in the UV.

The position angle of the intrinsic polarization in the U band ( $90^\circ \pm 10^\circ$ ) is not significantly different from that in the UV ( $81^\circ \pm 10^\circ$ ). The weighted mean position angle of the intrinsic component in the B through I bands is  $129^\circ \pm 11^\circ$ , which is significantly different from that in the UV ( $\Delta\theta_0 = 48^\circ \pm 14^\circ$ ). If the Rayleigh and Thomson scattering occur in physically separate regions, the polarizations induced by the two processes could have different position angles. The variation in position angle as a function of wavelength could then be caused by the different wavelength dependence of the scattering cross-section in the two processes. Thomson scattering would dominate in the B bandpass and at longer wavelengths, while Rayleigh scattering would dominate in the U bandpass and at shorter wavelengths.

Because the polarization is variable at all wavelengths, we can not obtain a meaningful estimate of the relative contributions of the two processes from our non-simultaneous observations.

There are other radiation mechanisms which can produce some of the properties of SS433 we observe in the UV, but require additional ad hoc hypotheses to explain them all. Impact ionization lines in the jets will be linearly polarized (Brown & Fletcher 1992), but only the relatively weak high-level Balmer lines will be Doppler-shifted into the F277M bandpass. The polarization in impact ionization lines is also unlikely to exceed a few percent, an order of magnitude less than the UV polarization we detect. Gyro-synchrotron radiation from the material in bulk motion in the precessing relativistic jets can produce UV radiation with the polarization and position angle we observe (Landau & Lifshitz 1959; Ramaty 1969). Radiation from monoenergetic electrons with  $v/c = 0.26$  is emitted primarily at a single frequency,  $\nu = 2.8 \times 10^6 H$  Hz, where the magnetic field strength,  $H$ , is in gauss. For  $\nu = 1.1 \times 10^{15}$  Hz, in the middle of the F277M bandpass,  $H \sim 4 \times 10^8$  G in the region producing the radiation. Although magnetic fields as large as  $10^{12}$  G have been inferred to exist near neutron stars (Trumper et al. 1978), a magnetic field as large as  $4 \times 10^8$  G is unlikely to exist in the relativistic jets from which the gyro-synchrotron radiation would be emitted.

Another mechanism which might operate in SS433 involves collimated electron-positron beams directed along the jets, suggested to occur for theoretical reasons (Lovelace & Ruchti 1983). When eventually stopped in the jets, the positrons would form positronium atoms. The positronium-Lyman  $\alpha$  line at 2340 Å would be redshifted into our F277M bandpass if the material in which the positrons are stopped took part in the semi-relativistic motion of the material in the precessing jet. The radiation in the line would be unpolarized, however, requiring an additional mechanism to polarize it. Zeeman splitting of positronium-Ly  $\alpha$  into three linearly polarized components when viewed perpendicular to a strong magnetic field would not produce a polarized signal in our analyzer unless only one component of the normal Zeeman triplet were shifted into our 340 Å wide bandpass. Decreases in  $p$  would then be caused by this Zeeman component being shifted out of the F277M bandpass by precession of the jets. Such a correlation between  $p$  and  $\psi$  is not observed, however. In addition, neither gyro-synchrotron emission nor Zeeman splitting of positronium-Ly  $\alpha$  would produce simultaneously the large polarization we observe in both the U bandpass and in the UV.

Rayleigh scattering appears to be the only physically plausible mechanism for generating the wavelength dependence of polarization we observe in SS433.

#### 4.2. Photometry

The UV flux observed from SS433 at the phases of the bright and low states given in Sect. 3.3 is shown in Fig. 6 together with that reported in the literature in the U, B, V, and R bandpasses as evaluated by Panferov et al. (1997). We caution that the fluxes in the other bandpasses were obtained at a different epoch from our

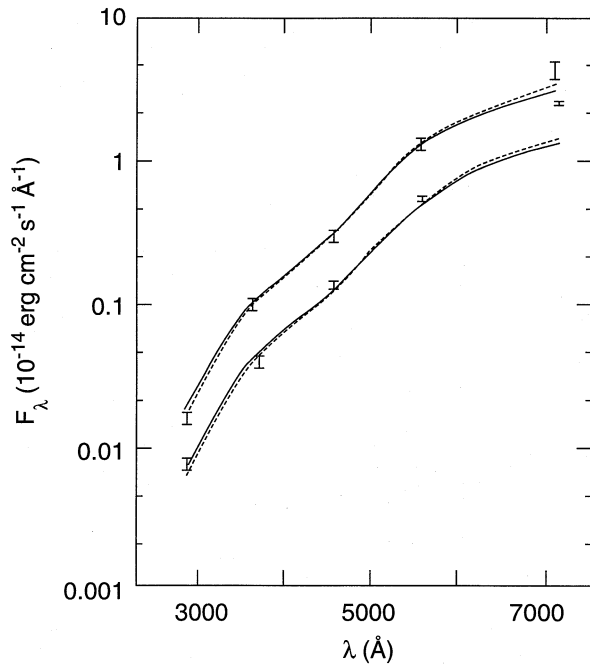


**Fig. 6.** The flux observed from SS433 in the F277M bandpass together with the fluxes in the U, B, V, and R bandpasses compiled by Panferov et al. (1997). Above: in the bright state; below: in the low state. The fluxes are shown at their isophotal wavelengths, which take the slope of the SS433 spectrum into account. The UV fluxes were observed at a different epoch from the others. The solid line is the minimum  $\chi^2$  representation of the UVB data alone by a single-temperature black body reddened by interstellar absorption; the dotted line, of the UV plus UVB data.

F277M observations. The observed fluxes can be represented by a single-temperature black-body spectrum reddened by the interstellar absorption found by O'Donnell (1994) and Cardelli et al. (1989). The best fitting black-body spectrum to the UVB data alone is shown as a solid line in Fig. 6 for the two different brightness states; the dotted line is the best fitting representation to these three bandpasses plus the UV data. The R band data were not included in the fitting procedure because some evidence exists of a significant contribution in that band from a free-free emission source (Panferov et al. 1997). We note that even a single black body derived solely from the optical data predicts the UV data reasonably well.

An acceptable representation of the bright state fluxes ( $\chi^2 = 2.65$  for 2 degrees of freedom), occurs for  $T = (7.2 \pm 2.0) \times 10^4$  K and  $A_V = 8.4(+0.2, -0.3)$ . No acceptable representation was found for the low state. A typical unacceptable representation (minimum  $\chi^2 = 25.6$ ) gives  $T = 4.9(+2.9, -1.5) \times 10^4$  K and  $A_V = 8.2 \pm 0.5$ . In both states, the radius of the black body is  $(1.5 - 2.0) \times 10^{12}$  cm at a distance of 5.1 kpc. We will reserve further discussion of these results to a separate paper.

## 5. Conclusions

The UV polarization observed from SS433 is both large ( $\langle p \rangle = 13 \pm 4\%$ ) and variable. An intrinsic component of

polarization must dominate the polarization in the UV. The increase in polarization in SS433 from the visible into the UV requires its intrinsic polarization to be strongly wavelength dependent. If scattering is the mechanism producing the intrinsic polarization, then it must contain a significant component caused by Rayleigh scattering. SS433 would then join Cygnus XR-1, 4U0900-40, and 4U1700-37 as an X-ray emitting binary system in which combined Rayleigh and Thomson scattering has been identified as a source of optical polarization (Wolinski et al. 1996). At  $\psi = 0.131$ , less than 1.2% of the flux from SS433 ( $3\sigma$  upper limit) is modulated with any period between 200  $\mu$ s and 100 s.

*Acknowledgements.* We thank G. D. Holman and R. J. Drachman for calculations of the polarization and spectrum of gyro-synchrotron radiation. The High Speed Photometer Investigation Definition Team is supported by NASA contract NAG 5-1613 to the University of Wisconsin. PTB was supported by NASA contract NAS 5-32484 to USRA.

## References

- Arav N., Begelman M. C., 1993, ApJ 413, 700
- Bjorkman J. E., Bjorkman K. S., 1994, ApJ 436, 818
- Bjorkman K. S., Nordsieck K. H., Code A. D., et al., 1991, ApJ 383, L67
- Bless R. C., Percival J. W., Walter L. E., White R. L., 1992, High-Speed Photometer Instrument Handbook. STScI, Baltimore
- Boyd P. T., Carter P. H., Gilmore R., Dolan J. F., 1995, ApJ 445, 861
- Brown J. C., Fletcher, L., 1992, A&A 259, L43
- Cardelli J. A., Clayton G. C., Mathis J. S., 1989, ApJ 345, 245
- Cherepashchuk A. M., 1981 MNRAS, 194, 761
- Clarke D., Stewart B. G., Schwarz H. E., Brooks A., 1983, A&A 126, 260
- Dolan J. F., Tapia S., 1986, PASP 98, 792
- Dolan J. F., Boyd P. T., Wolinski K. G., et al., 1994, ApJ 432, 560
- Efimov Y. S., Piirola V., Shakhovskoy N. M., 1984, A&A 138, 62
- Fabrika S., 1993, MNRAS 261, 241
- Hjellming R. N., Johnston K. J., 1981, Nat 290, 100
- Kitamoto S., Miyamoto S., Tanaka Y., et al., 1984, PASJ 36, 731
- Krumenaker L. E., 1975, PASP 87, 185
- Landau L. D., Lifshitz E., 1959, The Classical Theory of Fields. Addison-Wesley, Reading, MA, Sec. 9-8
- Liebert J., Angel J. R. P., Hege E. K., Martin P. G., Blair W. P., 1979, Nat 279, 384
- Leibowitz E. M., Mendelson H., 1982, PASP 94, 977
- Lovelace R. V. E., Ruchti C. B., 1983, Positron-Electron Pairs in Astrophysics. AIP Press, New York, p. 314
- Margon B., 1984, ARA&A 22, 507
- Margon B., Anderson S. F., 1989, ApJ 347, 448
- Mason K.O., Hawkins F. J., Sanford P. W., Murdin P., Savage A., 1974, ApJ 192, L65
- McLean I. S., Tapia S., 1980, Nat 287, 703
- Meyer S. L., 1986, Data Analysis for Scientists and Engineers. Peer Managements Consultants, Evanston, IL, Chap. 25, 26
- Michalsky J. J., Stokes G. M., Szokdy P., Larson N. R., 1980, PASP 92, 654
- Newsom G. H., Collins II G. W., 1981, AJ 86, 1250
- Niell A. E., Lockhart T. G., Preston R. A., 1981, ApJ 250, 248
- O'Donnell J. E., 1994, ApJ 422, 158
- Panferov A. A., Fabrika S. N., 1993, Astron. Lett. 19, 41

- Panferov A. A., Fabrika S. N., Rakhimov V. Yu., 1997, *Astron. Rep.* 74, 392
- Percival J. W., Boyd P. T., Biggs, J. D. et al., 1995, *ApJ* 446, 832
- Ramaty R., 1969, *ApJ* 158, 753
- Rose W. K., 1995, *MNRAS* 276, 1191
- Serkowski K., 1974, *Planets, Stars and Nebulae Studied by Photopolarimetry* (ed. T. Gehrels). Univ. Arizona Press, Tucson, AZ, 170
- Simmons J. F. L., Stewart B. G., 1985, *A&A* 142, 100
- Stephenson C. B., Sanduleak N., 1977, *ApJS* 33, 459
- Stewart G. C., Watson M. G., Matsuoka M., et al., 1987, *MNRAS* 228, 293
- Taylor M., Code A. D., Nordsieck, K. H., et al., 1991, *ApJ* 382, L85
- Thompson R. I., Rieke G. H., Tokunaga A. T., Lebofsky M. J., 1979, *ApJ* 234, L135
- Trumper J., Pietsch W., Reppin C., et al., 1978, *ApJ* 219, L105
- Wagner R. M., 1986, *ApJ* 308, 152
- Wardle J. F. C., Kronberg P. P., 1974, *ApJ* 194, 249
- Wolinski K. G., Dolan J. F., Boyd P. T., et al., 1996, *ApJ* 457, 859

This article was processed by the author using Springer-Verlag L<sup>A</sup>T<sub>E</sub>X A&A style file L-AA version 3.